

Received:  
31 December 2013

Revised:  
21 May 2014

Accepted:  
3 June 2014

doi: 10.1259/bjr.20140024

Cite this article as:

Do RKG, McErlean A, Ang CS, DeMatteo RP, Abou-Alfa GK. CT and MRI of primary and metastatic fibrolamellar carcinoma: a case series of 37 patients. *Br J Radiol* 2014;87:20140024.

## FULL PAPER

# CT and MRI of primary and metastatic fibrolamellar carcinoma: a case series of 37 patients

<sup>1,2</sup>R K G DO, MD, PhD, <sup>1,2</sup>A MCERLEAN, MBCh, BAO, <sup>2,3</sup>C S ANG, MD, <sup>2,4</sup>R P DEMATTEO, MD and <sup>2,3</sup>G K ABOU-ALFA, MD

<sup>1</sup>Department of Radiology, Memorial Sloan Kettering Cancer Center, New York, NY, USA

<sup>2</sup>Weill Medical College at Cornell University, New York, NY, USA

<sup>3</sup>Department of Medicine, Memorial Sloan Kettering Cancer Center, New York, NY, USA

<sup>4</sup>Department of Surgery, Memorial Sloan Kettering Cancer Center, New York, NY, USA

Address correspondence to: Dr Richard K. G. Do

E-mail: [dok@mskcc.org](mailto:dok@mskcc.org)

**Objective:** Fibrolamellar carcinoma (FLC) is a rare disease, with limited radiographic reported information. We assessed the imaging patterns of primary and metastatic FLC.

**Methods:** CT and MR examinations of patients with FLC were retrospectively reviewed. Imaging features were assessed for primary and recurrent liver tumours, including dimension, enhancement characteristics, and presence or absence of central scars. Locations of nodal and extranodal metastases were also recorded.

**Results:** Of 37 patients (18 males and 19 females; average age, 23.5 years) with FLC, 24 had imaging of their primary tumour; 13 had metastases at presentation and 7 developed metastases on follow-up. The remaining 13 patients had follow-up imaging of metastatic disease. Primary FLC had a mean diameter >11cm, with central scars in ten (46%) patients. Most tumours enhanced heterogeneously (96%) and showed arterial enhancement

(81%). On MRI, 62% of FLCs were hypointense on  $T_1$  weighted imaging and 54% were hyperintense on  $T_2$  weighted imaging. 13 patients (54%) had nodal metastases at presentation, mostly in the upper abdomen (92%) and commonly in the chest (38%). Extrahepatic metastases were most frequently pulmonary or peritoneal. Predominantly small and homogeneous intrahepatic recurrences were detected on follow-up in 15 patients.

**Conclusion:** FLC often presents as a large hepatic tumour with nodal and distant metastases. Thoracic adenopathy and lung metastases were frequently found in our series, suggesting the need for pre-operative and follow-up chest imaging.

**Advances in knowledge:** Thoracic nodal and lung metastases are common in FLC; therefore, dedicated chest imaging should be part of the evaluation of a patient with FLC.

Fibrolamellar carcinoma (FLC) is a rare and distinct disease from hepatocellular carcinoma (HCC). It accounts for <1% of primary liver malignancies.<sup>1</sup> Compared with conventional HCC, FLC is often found in younger patients, may be slightly more prevalent in females and typically occurs in the absence of cirrhosis or risk factors such as viral hepatitis, alcohol abuse or non-alcoholic fatty liver disease.<sup>1-3</sup>

The prognosis of FLC is not fully understood. Median survival in patients with resectable disease is as high as 112 months, and a 10-year survival rate of 70% has been reported.<sup>4,5</sup> The improved prognosis in some patients may be attributable to the absence of chronic liver disease, as patients with HCC in the absence of cirrhosis share a similar prognosis.<sup>2,6,7</sup> Despite curative resection, however, recurrences are common and are often removed surgically where possible given the lack of other effective therapies.<sup>6</sup> Patients with advanced or unresectable FLC

have a very poor prognosis, with a 5-year survival rate of 0-15% and a median survival of 5-12 months.<sup>2-5</sup> Serious attempts are being taken to help find effective therapy for this disease.<sup>8</sup> Oestrogen suppression and mammalian target of rapamycin inhibition, two novel therapeutic strategies designed specifically for FLC, are currently being evaluated in a randomized Phase II clinical trial conducted by the FLC Consortium at Memorial Sloan Kettering Cancer Center, New York, NY; University of California, San Francisco, San Francisco, CA; Johns Hopkins University, Baltimore, MD; Dana Farber/Children's Hospital Cancer Center, Boston, MA; Massachusetts General Hospital, Boston, MA; and University of Texas Southwestern, Dallas, TX.

Imaging features of FLC on both CT and MRI have previously been reported.<sup>9-14</sup> It frequently presents as a large, well-demarcated and lobulated liver mass that can contain

a central scar and calcifications. The fibrolamellar name refers to sheets of fibrous tissue separating neoplastic cells, which can coalesce and form a central scar, a helpful imaging characteristic of this rare tumour. Patterns of metastatic disease for FLC have also been described previously.<sup>12,14</sup> Nodal metastases in the abdomen are relatively common, whereas thoracic nodal metastases appear to be rare. Peritoneal spread seems to be the most common pattern of extranodal disease, with lung and adrenal metastases occurring occasionally. Radiologists can play a role in the management of this rare tumour, both by raising the possibility of its diagnosis and by identifying the metastatic disease at presentation or during follow-up, which may help in deciding the appropriate therapy in this rapidly evolving field.

In this study, we retrospectively reviewed the CT and MRI findings of primary as well as metastatic FLC in 37 patients who were seen at Memorial Sloan Kettering Cancer Center and investigated the patterns of metastatic disease.

## METHODS AND MATERIALS

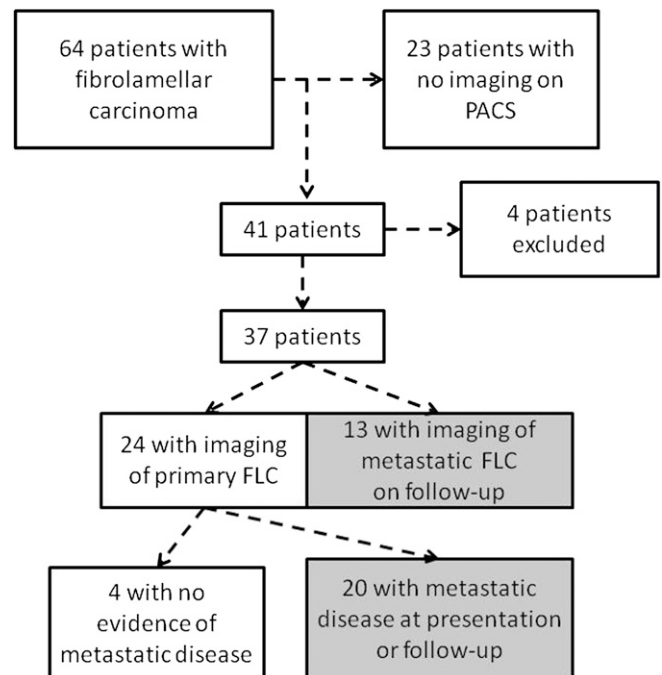
A waiver of consent was obtained from the institutional review board for this retrospective review. 64 patients were identified from a search of the pathological database for FLC, treated at the Memorial Sloan Kettering Cancer Center between January 1985 and December 2010. Among these, 41 patients had imaging on picture archiving computer systems (PACS, Centricity™; GE Healthcare Integrated Imaging Solutions, Wauwatosa, WI) available for review, 1 of whom was excluded because they had a mixed tumour histology, 2 of whom were excluded for poor quality imaging of their primary tumour, and 1 of whom was excluded because there was no imaging of the primary tumour, and no evidence of recurrence on any follow-up imaging examination.

### Imaging technique

There was a wide variation in imaging modalities, type of intravenous contrast used, phases of contrast enhancement included and MR sequences used owing to changes in imaging technique that occurred between the first study available for review in 1999 and 2011 and owing to a number of studies that were performed at outside institutions. For 20 CT examinations of primary liver tumours, 4 studies were available only on film that was scanned into PACS. One included portal venous phase (PV) imaging alone, one consisted of non-contrast (NC) and PV, one included arterial phase (ART) and PV and the last included a triple phase CT (NC, ART and PV). Of the remaining 16 patients, 9 had triple phase CT imaging available, 5 had PV imaging alone, 1 had NC and ART imaging and 1 had NC and PV imaging available. The iodinated contrast agents, rate of contrast injection and timing of arterial and portal venous phases were not always available.

For 13 MRI examinations of primary liver tumours, a single study was only available on film that was scanned into PACS. For the remaining 12 MRI examinations, all were performed on 1.5-T scanners, using a variety of gadolinium-based contrast agents that were not always specified, but only 1 study was performed with a hepatobiliary contrast agent, gadoxetate disodium

(Gd-EOB-DTPA, Eovist®/Primovist™; Bayer HealthCare, Leverkusen, Germany), and included delayed hepatobiliary imaging. All 12 studies included gradient echo  $T_1$  weighted ( $T_1w$ ) sequences, with repetition time (TR) range of 100–200 ms for two-dimensional and 7.6–7.7 ms for three-dimensional sequences, and echo time (TE) = 1.8–2.4 ms for opposed phase imaging and 4.2–5.2 ms for in-phase imaging. All 12 studies included fast (turbo) spin echo (FSE)-based  $T_2$  weighted ( $T_2w$ ) imaging, with or without fat saturation, including 9 with a conventional TR range of 2317–4600 ms and TE from 98 to 140 ms. The remaining three studies included a respiratory-triggered  $T_2w$  FSE sequence with TR = 12,000 ms; TE = 99 ms, a single shot FSE with TE = 395 ms, and a  $T_2w$  FSE with fat saturation with TR = 370 ms; TE = 80 ms.



(Gd-EOB-DTPA, Eovist®/Primovist™; Bayer HealthCare, Leverkusen, Germany), and included delayed hepatobiliary imaging. All 12 studies included gradient echo  $T_1$  weighted ( $T_1w$ ) sequences, with repetition time (TR) range of 100–200 ms for two-dimensional and 7.6–7.7 ms for three-dimensional sequences, and echo time (TE) = 1.8–2.4 ms for opposed phase imaging and 4.2–5.2 ms for in-phase imaging. All 12 studies included fast (turbo) spin echo (FSE)-based  $T_2$  weighted ( $T_2w$ ) imaging, with or without fat saturation, including 9 with a conventional TR range of 2317–4600 ms and TE from 98 to 140 ms. The remaining three studies included a respiratory-triggered  $T_2w$  FSE sequence with TR = 12,000 ms; TE = 99 ms, a single shot FSE with TE = 395 ms, and a  $T_2w$  FSE with fat saturation with TR = 370 ms; TE = 80 ms.

### Image analysis

CT and MR images were reviewed on PACS in consensus by two radiologists (RKD and AM). The following imaging characteristics were recorded for primary liver tumours: number of tumours and size of the largest tumour; the presence or absence of the following morphological characteristics: central scar, fat, haemorrhage, gross vascular invasion and biliary dilatation. For patients with only imaging available on film scanned to PACS, measurements were performed after calliper calibration. The presence of calcifications was assessed for those with available CT images. On pre- and dynamic post-contrast imaging, the

Table 1. Pre-operative imaging of fibrolamellar carcinoma

Patient	Age (years)/sex	Imaging techniques <sup>a</sup>	Size (cm)	Imaging features <sup>b</sup>	Lymphadenopathy <sup>c</sup>	Short axis (cm)	Metastases <sup>d</sup>	Ascites <sup>e</sup>	Pre-operative treatment <sup>e</sup>
1	28/M	MRI	12.6	H	TP	1.1	0	Y	
2	39/F	CT	8.5		TN		0	Y	
3	20/M	CT	17.7	H, C, S	TP	4.9	0		
4	34/M	CT + MRI	9.3		FN		0		
5	17/M	CT + MRI	11.9	C, S	FP	2.0	0		
6	23/M	CT	18.3	V	TP	3.5	IH, Lu, per, Pleu	Y	
7	20/F	CT	13.2	B, C, S	TP	7.4	0	Y	
8	13/M	CT	13.6		FP	1.5	Lu	Y	Y
9	30/M	CT	10.2	B, C, S	TN		0		
10	20/M	CT	15.9	B, C, S	TP	4.2	0	Y	
11	17/F	CT	6.2		TN		0		
12	15/F	CT	7.6	B, S	TP	5.4	Per	Y	Y
13	24/M	CT + MRI	17.0	H, C, S	TN		0		
14	17/M	CT + MRI	11.5	C, S	FN		0		
15	16/F	MRI	4.8	C, S	TN		0		
16	18/F	CT	11.7		FN		0		
17	18/M	CT	14.0	B	TP	8.6	IH		
18	19/F	CT + MRI	6.1	B	TP	2.8	0		Y
19	39/M	CT	10.3		TP	2.5	Per		
20	16/F	MRI	11.9		TN		Lu, per		
21	27/F	MRI	9.7		TN		0		
22	22/F	CT	15.0	V, S	TP	4.2	0		Y
23	14/F	CT + MRI	12.3	B	FP	1.8	0		
24	15/F	CT + MRI	13.1	B, C, S	TP	2.3	Lu		

F, female; M, male.

<sup>a</sup>Imaging techniques include CT or MRI.

<sup>b</sup>Imaging features assessed include biliary dilatation (B), haemorrhage (H), calcifications (C), scar (S) and gross vascular invasion (V).

<sup>c</sup>Lymphadenopathy (LAD) was classified as true positives (TPs), true negatives (TNs), false positive (FP) or false negative (FN) based on our reference standard.

<sup>d</sup>Metastases were either intrahepatic (IH) or found in the lungs (Lu), peritoneum (Per) or pleura (Pleu).

<sup>e</sup>Ascites and pre-operative treatment was noted when present (Y = yes).

homogeneity vs heterogeneity of the tumour and its enhancement compared with adjacent liver parenchyma was recorded on ART imaging. On MRI, signal intensity of the tumours on T1w, T2w and diffusion-weighted imaging (DWI) sequences were recorded when available. The same imaging parameters were used to assess for intrahepatic recurrences or metastases. Extrahepatic nodal and distant metastases were evaluated at pre-operative imaging and on follow-up imaging.

#### Reference standard

Patients' electronic medical records were reviewed for pathological reports, to confirm the diagnosis of FLC. Pathological reports were reviewed for confirmation of a central scar. When nodal sampling was performed at surgery, histopathological

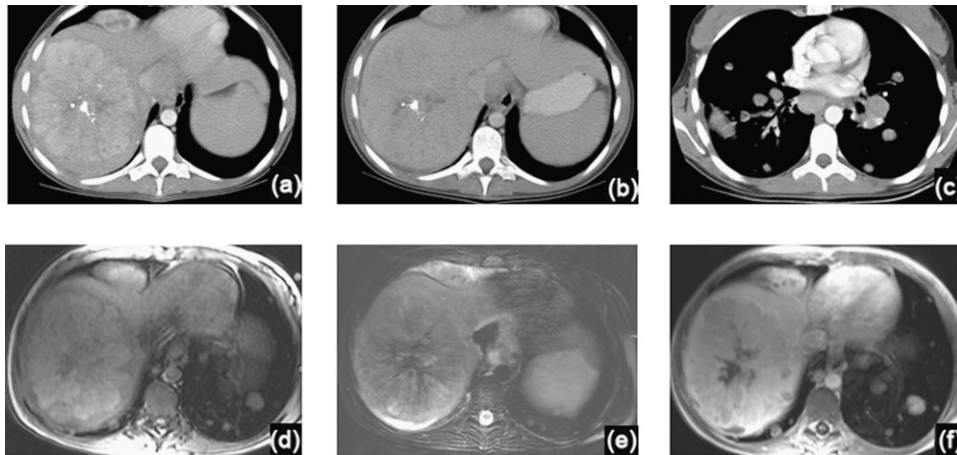
evidence of nodal metastasis was also recorded. In the absence of pathological proof for metastatic disease, a short axis diameter >1 cm in combination with unresectable disease or interval growth was used as a criterion for nodal metastases; pathological confirmation, interval growth on serial imaging or characteristic appearance in the setting of unresectable disease was used as a reference standard for non-nodal metastases.

## RESULTS

### Patient demographics

We studied 37 patients with an average age of 23.5 years (range, 13–48 years). 11 (30%) were below 18 years of age. There was a nearly even distribution of patients between both genders, 18 male (49%) and 19 female (51%) patients. Among

Figure 2. A 15-year-old female with primary fibrolamellar carcinoma (FLC). (a–c) Intravenous contrast-enhanced CT axial images through the liver (a, b) and chest (c), demonstrate a large right hepatic FLC with typical imaging features, including heterogeneous hypervascularity during the arterial phase (a) and a central scar with calcifications. FLC remains heterogeneous on the portal venous phase, with attenuation similar to liver parenchyma (b). In the chest, mediastinal and hilar adenopathy as well as lung metastases are evident (c). (d–f) Axial MR images through the liver, before (d, e) and after intravenous contrast administration (f), demonstrate a right hepatic FLC with heterogeneous signal predominantly similar to liver parenchyma on  $T_1$  weighted (d) and  $T_2$  weighted (e) sequences. The central scar is heterogeneously hypointense on  $T_1$  and  $T_2$  weighted images, with lack of enhancement on contrast-enhanced images (f).



the 37 patients, 24 patients (65%) had imaging of their primary tumour, while the remaining 13 patients had only post-operative imaging of metastatic FLC on follow-up (Figure 1). 32 of 37 patients had pathology of their primary tumour established at surgery, 4 patients with unresectable disease had percutaneous biopsy performed and a single patient had pathological confirmation of a surgically resected liver recurrence. Four patients underwent pre-operative treatment with different forms and combinations of systemic and locoregional therapy including chemotherapy, biologic therapy, chemotherapy plus radiation therapy and chemo-embolization. 20 (83%) of the 24 patients with pre-operative imaging had evidence of metastatic disease at presentation or

during subsequent follow-up. A total of 33 patients had imaging of metastatic FLC.

Imaging features of primary fibrolamellar carcinoma  
Imaging of primary FLC was available for 24 patients; 11 only had CT imaging, 4 only had MRI and 9 had both CT and MRI examinations. The imaging findings are summarized in Table 1. Patients typically presented with a large primary FLC in a liver without imaging evidence of cirrhosis. The mean size of the primary tumour was 11.8 cm (range, 4.8–17.7 cm). In patients who had available multiphasic CT or MRI, primary FLC commonly demonstrated hyperenhancement compared with adjacent liver parenchyma on ART (17/21 patients, 81%), and its

Figure 3. A 28-year-old male with primary fibrolamellar carcinoma. Axial MR images through the liver obtained before (a–c) and after intravenous contrast administration (d–f). Pre-contrast images demonstrate a large right posterior hepatic lobe tumour with heterogeneously hypointense signal on  $T_1$  weighted imaging (a) and hyperintense signal on  $T_2$  weighted imaging (b). This lesion remained hyperintense on axial fat-suppressed diffusion-weighted images with  $b = 800 \text{ s mm}^{-2}$  (c). On post-contrast  $T_1$  weighted imaging, this lesion was heterogeneously hypervascular during the arterial phase (d), with heterogeneous washout on portal venous phase (e). A satellite lesion was homogeneously hypervascular in Segment 7 more superiorly (f).

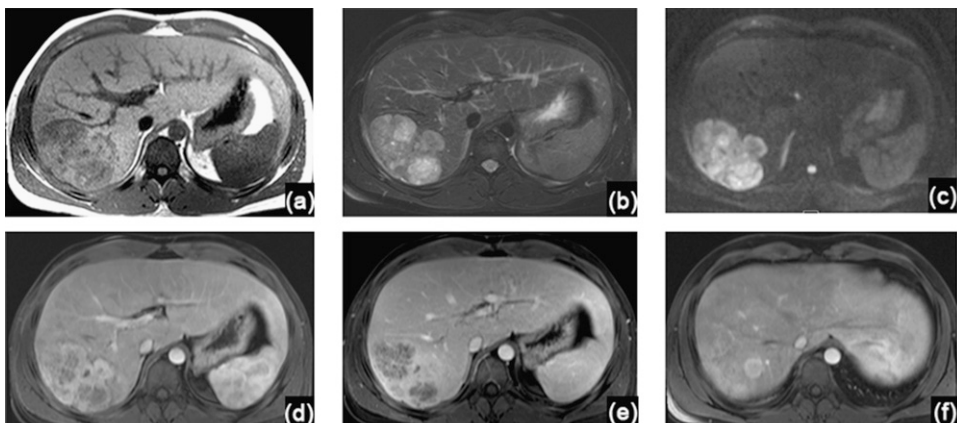
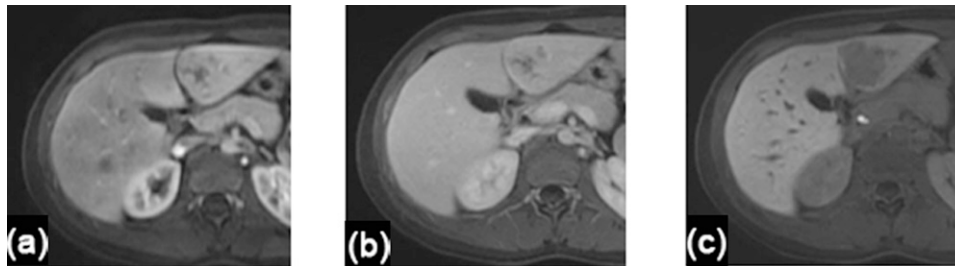


Figure 4. A 16-year-old female with primary fibrolamellar carcinoma. (a–c) Axial MR images through the liver demonstrate a left lateral segment tumour with heterogeneous enhancement on arterial phase (a) and portal venous phase (b). This lesion was uniformly hypointense on delayed hepatobiliary phase, 20 min after injection of gadoxetate disodium (Eovist®/Primovist™; Bayer HealthCare, Leverkusen, Germany) (c).



enhancement was heterogeneous in nearly all cases (23/24 patients, 96%) (Figure 2). The lone patient with a homogeneously enhancing primary tumour (Patient 18) had undergone prior chemotherapy and radiation therapy. A central scar is a feature of FLC that is helpful in its diagnosis and was found in 46% of our patients (Figure 2). When compared with pathological reports, only one additional patient was reported to have a scar that was not visible on imaging. For patients with both MR and CT imaging, when a central scar was seen on one modality, it was always seen on the other. Calcifications were seen in 9 (43%) out of 21 patients with CT imaging, with an associated central scar in each case (Figure 2). Delayed enhancement of the entire scar was never seen, but only three patients with scars had delayed imaging after the portal venous phase available for review. None of the primary FLC contained visible fat, and only three tumours had evidence of haemorrhage. Biliary dilatation was present in eight patients (33%) and gross vascular invasion was present in two patients (8%). Despite the absence of cirrhosis, seven patients (29%) presented with ascites.

In patients with MRI of their primary tumour, FLCs were hypointense in signal intensity on T1w imaging in 8 of 13 cases (62%) and hyperintense on T2w imaging in 7 of 13 cases (54%), when compared with the liver parenchyma (Figure 3). Central scars on MRI had a range of appearances, demonstrating either hypointensity or hyperintensity on both T1w and T2w images. High signal intensity of FLC was seen on DWI at high  $b$  values ( $\geq 500 \text{ s mm}^{-2}$ ). Since only two patients had available DWI using different sets of  $b$  values, the apparent diffusion coefficients of these tumours were not calculated for this study. In a single patient who underwent imaging pre-operatively with a hepatobiliary contrast agent, Gd-EOB-DTPA, FLC demonstrated heterogeneous hypointensity on delayed hepatobiliary phase imaging (Figure 4).

#### Patterns of metastatic fibrolamellar carcinoma

A total of 33 patients out of 37 (89%) had evidence of metastatic disease either at presentation or follow-up (Table 2). Four patients (Patients 9, 11, 15 and 23) had no evidence of metastatic disease at surgical resection and did not develop metastatic disease on follow-up. The patterns of intrahepatic, nodal and distant metastases will be discussed next for the 24 patients with imaging of their primary tumour and for the entire group of 33 patients with metastatic disease.

Of the 24 patients with imaging of their primary tumours, 2 (8%) had evidence of intrahepatic metastases at presentation (Table 2) in addition to nodal or distant metastases and were deemed to have unresectable disease. An additional 16 patients developed liver recurrences on follow-up, 8 of which (50%) occurred at the resection margin. Thus, out of 33 patients with metastatic disease, 18 (55%) developed intrahepatic metastases or recurrences at presentation or follow-up. The imaging characteristics of intrahepatic recurrences and metastases are summarized in Table 3. The majority of intrahepatic lesions were solitary (13/18, 72%), hypervascular (15/18, 83%) and small (13/18 <3 cm, 72%) (Figure 5). Five lesions were homogeneous in enhancement, and each one was <3 cm in size. A central scar was found in a single recurrence, which measured 5.9 cm. None of the recurrent liver tumours demonstrated calcifications or haemorrhage. Ten patients had pathological confirmation of intrahepatic recurrences, six patients were diagnosed by interval growth on imaging and two had initially unresectable disease as noted above.

FLC was often associated with enlarged abdominal or thoracic lymph nodes at presentation. Out of 24 patients with available pre-operative imaging, 14 (58%) had enlarged lymph nodes >1 cm in short axis at presentation (Table 1). 11 of these 14 patients had nodal metastases based on our reference standard: 5 had pathological confirmation from nodal sampling at initial surgery, 1 had interval growth with positive biopsy on follow-up within 7 months and 5 were deemed to have unresectable disease. The remaining three patients had negative lymph nodes dissections. Three out of ten patients who had no radiographically enlarged lymph nodes had nodal metastases confirmed at surgery. Thus, with a criterion of short axis >1 cm, CT and MRI had a sensitivity of 79% and specificity of 79% in our population. Of note, all ten patients with at least one lymph node with short axis >2 cm had nodal metastases by our reference standard. Out of the 11 patients with radiographically enlarged nodes who met our reference standard, 7 (64%) had abdominal adenopathy, 3 (27%) had both abdominal and thoracic adenopathy and 1 (9%) patient had only thoracic adenopathy (Figures 2 and 6). The nodes were more often heterogeneous in enhancement when larger.

We next explored the patterns of nodal metastases in our entire metastatic patient population of 33 patients, based on patients

Table 2. Patterns of metastatic disease

Patient	Age (years)/sex	Lymphadenopathy <sup>a</sup>		Metastases <sup>a</sup>				Local recurrence
		Abdominal	Chest	Peritoneal	Lung	Intrahepatic	Other	
1	28/M	P		F	F			F
2	39/F					F	Bone	
3	20/M	P						
4	34/M	P		F				
5	17/M	F		F				F
6	23/M	P	P	P	P	P	Pleura	
7	20/F	P	P					
8	13/M				P			
10	20/M	P	P					F
12	15/F	P		P				
13	24/M					F		
14	17/M	P						F
16	18/F	P						
17	18/M	P				P		
18	19/F	P		F		F		
19	39/M	P		P				F
20	16/F	F		P	P	F		
21	27/F							F
22	22/F	P						
24	15/F	P	P		P			
25	16/F	P			F	F		
26	24/F		F		F			
27	20/M	P			F			F
28	32/M	F		F				
29	30/F		F		F			
30	26/F			P			Pericardial	
31	23/F	P				F		
32	38/F	P				F		
33	31/F				F	F		
34	20/M	F	F	P	F			
35	17/M	F	F					
36	48/M	F						F
37	24/M			F				

F, female; M, male.

<sup>a</sup>Lymphadenopathy or metastatic disease was noted either at presentation (P) or on follow-up (F).

who met our reference standard. Out of these 33 patients, 25 patients (76%) had nodal metastases, 17 of 25 (68%) were found to have nodal metastases at the time of their initial surgery (including patients who did not have pre-operative imaging) and the remaining 8 (32%) developed nodal metastases on follow-up (Table 2). Of these 25 patients with nodal metastases,

17 (68%) demonstrated only abdominal lymphadenopathy, 6 (24%) had both abdominal and thoracic lymphadenopathy and 2 (8%) patients developed only thoracic lymphadenopathy. In this group of 25 patients, 18 had pathological confirmation of nodal metastases, 6 had unresectable disease at presentation (Patients 6, 7, 17, 22, 24 and 35) and 1 had interval growth of

Table 3. Imaging of recurrent and intrahepatic metastatic fibrolamellar carcinoma

Patient	Age (years)/sex	Imaging technique <sup>a</sup>	Size (cm)	Surgical margin recurrence	Time interval (years)
1	28/M	CT	1.7	Yes	1.09
2	39/F	CT	2.7		1.04
5	17/M	MRI	1.0	Yes	6.86
6	23/M	CT	2.8		0
10	20/M	CT	2.2	Yes	1.36
13	24/M	CT	5.9		0.69
14	17/M	MRI	4.6	Yes	1.58
17	18/M	CT	2.1		0
18	19/F	CT + MRI	1.6		0.39
19	39/M	CT	1.4	Yes	4.35
20	16/F	CT	4.6		0.30
21	27/F	MRI	1.4	Yes	0.65
25	16/F	CT	10.5		2.94
27	20/M	MRI	2.1	Yes	1.42
31	23/F	CT	5.6		0.25
32	38/F	CT	2.0		5.84
33	31/F	CT	1.0		4.22
36	48/M	CT	2.2	Yes	6.87

F, female; M, male.

<sup>a</sup>Imaging techniques include CT or MRI.

lymph nodes as well as extrahepatic metastases on follow-up (Patient 20).

Distant metastases were found in 20 out of 33 patients (61%), 8 out of 20 (40%) at presentation and 12 out of 20 (60%) during follow-up, most commonly to the lung and peritoneum (Table 2). Of these 20 patients with distant metastases, 7 (35%) demonstrated peritoneal metastases, 7 (35%) demonstrated lung metastases and 3 (15%) had both peritoneal and lung metastases. An additional patient with both peritoneal and lung metastases also had pleural metastases at presentation (Figure 7). One patient developed peritoneal and pericardial metastases, while a single patient developed metastatic disease only to the bone during follow-up, which was discovered while being treated at another institution. 13 patients had pathological

confirmation of metastatic disease, 2 had unresectable disease at presentation and 4 had enlarging metastatic disease to the lung and/or peritoneum with a classic appearance. The patient with metastatic disease to bone was not pathologically confirmed.

Overall, in our entire cohort of 37 patients, 20 developed distant metastases (54%) either at presentation or follow-up, including 12 patients (32%) with peritoneal metastases and 11 (30%) with lung metastases. Patients with ascites at initial presentation (Table 1) did not necessarily have peritoneal metastases at presentation or during follow-up. Two out of seven patients with ascites at presentation had visible peritoneal tumours, and one of these seven patients developed peritoneal metastases on follow-up. No adrenal metastases were seen in any of our 37 patients.

Figure 5. A 40-year-old female with fibrolamellar carcinoma intrahepatic recurrence. (a–c) Axial MR images through the liver before (a) or after intravenous contrast administration during the arterial phase (b) or portal venous phase (c) demonstrate a low attenuation mass near the hepatic resection margin. This mass demonstrates homogeneous arterial enhancement (b) and is nearly isodense to surrounding liver on portal venous phase (c).

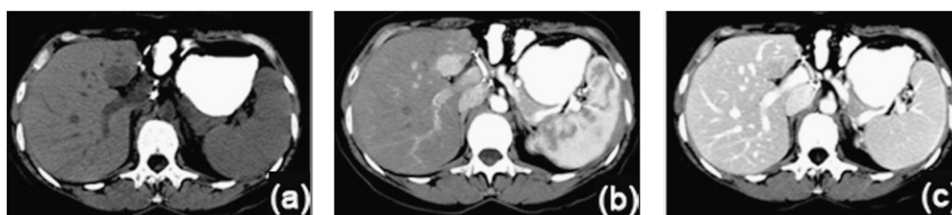
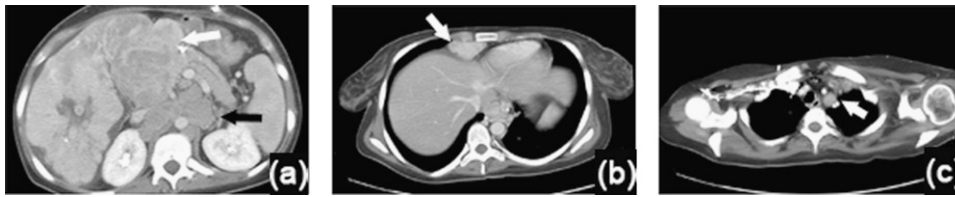


Figure 6. A 20-year-old female with fibrolamellar carcinoma (FLC) nodal metastases. (a–c) Intravenous contrast-enhanced axial CT images through the liver (a, b) and chest (c), demonstrate a right hepatic FLC containing a central scar, with enlarged, heterogeneous nodal metastases to the porta hepatis (white arrow) and smaller homogeneous para-aortic nodes (black arrow) (a). Additional supradiaphragmatic adenopathy (arrow) (b) and mediastinal adenopathy (arrow) (c) were present.



## DISCUSSION

Our results illustrate the variable appearance of primary and metastatic FLC in a series of 37 patients treated at the Memorial Sloan Kettering Cancer Center and are generally consistent with those described in the previous literature.<sup>9–14</sup> These tumours typically arise in a non-cirrhotic liver as a large solitary lesion that enhances heterogeneously. A central scar was found in nearly half (46%) of our patients and may be helpful in the diagnosis of this rare tumour. In the prior literature, central scars were found in the majority of tumours 55–71%,<sup>10–15</sup> except in one series dating back to 1985 when cross-sectional imaging was not routinely available and central scars were found in only two out of ten patients.<sup>10</sup>

In our series, FLC often metastasized to lymph nodes of the abdomen and chest, and these nodal metastases were often confluent and large. Similar to previous reports,<sup>11,13</sup> over half (58%) of our patients with pre-operative imaging of FLC presented with enlarged lymph nodes on CT or MRI. In our study, the specificity for metastatic lymphadenopathy pre-operatively was 79% when using a lymph node size criteria of >1 cm in short axis diameter on CT or MRI. We also found that all patients with at least one lymph node with short axis >2 cm were found to have metastatic lymphadenopathy based on our reference standard. All patients with CT or MRI demonstrating multiple lymph nodes >1 cm in short axis were found to have metastatic FLC at histopathological examination in a previous study.<sup>12</sup> Thus, the positive predictive value of lymphadenopathy on pre-operative imaging seems to be high for this patient population, in contrast to patients with conventional HCC who often have reactive lymphadenopathy. However, all these findings would require validation in larger prospective series. In addition, nodal metastases in the chest occurred in approximately 25% of our patients who had metastatic disease, contrasting with prior case series reporting a lower frequency in the range of 6–10%, or reported as unusual case reports.<sup>12,14,16,17</sup> Since

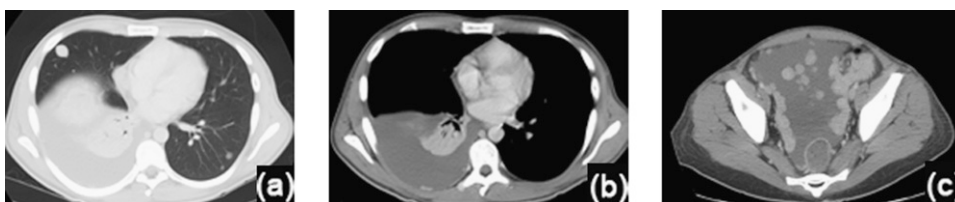
resection is currently the only effective treatment for this population, alerting the referring clinician to the presence of suspicious lymphadenopathy and considering pre-operative imaging of the chest may be helpful for staging and treatment planning.

Based on our results, FLC metastasizes to the lungs and peritoneum with nearly equal frequency. Both lung and peritoneal metastases from FLC were previously reported in a series of 40 patients, where 2 patients were reported to have peritoneal metastases and 9 had lung metastases.<sup>12</sup> While pulmonary and peritoneal metastases are also common in conventional HCC, osseous and adrenal metastases that are commonly found in patients with metastatic HCC<sup>18</sup> were rare in our FLC population.

In contrast to primary FLC, liver recurrences in our series were often small and more often homogeneous in enhancement, with the vast majority lacking calcifications or a central scar. These findings differ from those of two prior studies where liver recurrences were larger (average, 6 cm)<sup>14</sup> and often contained a central scar (50–57%).<sup>12,14</sup> Our discrepant results could potentially be explained by a shorter time interval between follow-up imaging studies in our patient population, possibly resulting in the earlier detection of smaller recurrences, and obviously the small sample sizes.

Although CT is adequate for initial pre-operative imaging of FLC, especially for evaluation of the thorax for nodal and pulmonary metastases, MRI may be helpful for initial work-up when FLC is first discovered as an incidental liver mass. The main differential diagnosis for FLC includes other hypervascular liver lesions, including benign entities such as focal nodular hyperplasia (FNH), and hepatic adenomas, as well as malignant masses such as conventional HCC and hypervascular liver metastasis. The commonest diagnostic dilemma for radiologists is to distinguish FLC from either FNH or conventional HCC, where both can present as large solitary liver masses with

Figure 7. A 23-year-old male with fibrolamellar carcinoma distant metastases. (a–c) Intravenous contrast-enhanced axial CT images through the chest (a, b) and pelvis (c), demonstrate pulmonary metastases (a), a small right posterior pleural metastasis with associated pleural effusion, and extensive pelvic peritoneal metastases with ascites (c).





a central scar. As previously reported, FLC frequently has a low signal on T1w and a high signal on T2w images compared with normal liver parenchyma, which are distinguishing characteristics from FNH.<sup>11,13</sup> MRI may also be more helpful than CT in the detection of central scars. FNH and FLC share similar features such as a central scar, but unlike FNH, the central scar in FLC does not always enhance on delayed images.<sup>13,19</sup> The role of hepatobiliary MR contrast agents is unclear at this time but is potentially helpful if FLCs are hypointense on delayed hepatobiliary phase imaging in contrast to the majority of FNHs, as was seen in one of our patients and in the reported literature.<sup>20,21</sup> Conventional HCCs typically do not contain a central scar, although a minority (6%) can in the setting of cirrhosis.<sup>22</sup> The central scar in FLC is also typically hypointense on both T1w and T2w imaging<sup>11,15</sup> but has also been reported as hyperintense on T2w imaging, similar to our experience, and similar to scars in FNH.<sup>23</sup> Of note, in a study comparing tumours with central scars, including FLC, FNH and haemangiomas, radiologists were able to distinguish FLC from FNH with high accuracy.<sup>24</sup> Thus, the absence of delayed enhancement along with hypointensity of a central scar on T2w imaging in a large mass that is not uniformly iso-intense to liver parenchyma should raise the suspicion of FLC. Other imaging characteristics such as calcifications on CT and heterogeneity of enhancement can further help in the diagnosis of FLC.

This study is limited by the retrospective nature of the data with several imaging studies on PACS originating from outside institutions, where precise imaging protocols such as contrast

type and rate of injection and timing could not be retrieved. In combination with the large time span of cases from 1985 to 2011, there was a lack of uniform imaging protocols for both CT and MRI. The lack of uniform imaging on CT did not limit our ability to measure lymph nodes or identify metastatic disease to the lungs and peritoneum. Assessment of FLC imaging features was performed in consensus; interobserver variability in detection of FLC imaging characteristics was not calculated in this retrospective study. However, this retrospective study was not performed to address the accuracy of CT and MRI in distinguishing FLC from other liver tumours. This study is also limited by the lack of pathological confirmation for all nodal metastases, intrahepatic recurrences and extrahepatic metastases. Nevertheless, the majority of patients with metastatic disease were confirmed pathologically.

## CONCLUSIONS

The imaging features of primary FLC in our series are generally consistent with those reported in the prior literature, with a few exceptions. Our series had a lower frequency of central scars and calcifications than previously reported, especially in the imaging of recurrent disease in the liver. This finding is possibly owing to differences in imaging technique across studies. We also found thoracic nodal metastases and lung metastases more frequently, highlighting the importance of thoracic imaging during initial treatment planning as well as for post-operative follow-up. Raising the suspicion of nodal metastases is crucial for the interpreting radiologist since surgical resection remains the treatment of choice at this time.

## REFERENCES

1. El-Serag HB, Davila JA. Is fibrolamellar carcinoma different from hepatocellular carcinoma? A US population-based study. *Hepatology* 2004; **39**: 798–803. doi: 10.1002/hep.20096
2. Kakar S, Burgart LJ, Batts KP, Garcia J, Jain D, Ferrell LD. Clinicopathologic features and survival in fibrolamellar carcinoma: comparison with conventional hepatocellular carcinoma with and without cirrhosis. *Mod Pathol* 2005; **18**: 1417–23.
3. Moreno-Luna LE, Arrieta O, Garcia-Leiva J, Martinez B, Torre A, Uribe M, et al. Clinical and pathologic factors associated with survival in young adult patients with fibrolamellar hepatocarcinoma. *BMC cancer* 2005; **5**: 142. doi: 10.1186/1471-2407-5-142
4. Hemming AW, Langer B, Sheiner P, Greig PD, Taylor BR. Aggressive surgical management of fibrolamellar hepatocellular carcinoma. *J Gastrointest Surg* 1997; **1**: 342–6.
5. Stipa F, Yoon SS, Liau KH, Fong Y, Jarnagin WR, D'Angelica M, et al. Outcome of patients with fibrolamellar hepatocellular carcinoma. *Cancer* 2006; **106**: 1331–8. doi: 10.1002/cncr.21703
6. Katzenstein HM, Krailo MD, Malogolowkin MH, Ortega JA, Qu W, Douglass EC, et al. Fibrolamellar hepatocellular carcinoma in children and adolescents. *Cancer* 2003; **97**: 2006–12. doi: 10.1002/cncr.11292
7. Ringe B, Wittekind C, Weimann A, Tusch G, Pichlmayr R. Results of hepatic resection and transplantation for fibrolamellar carcinoma. *Surg Gynecol Obstet* 1992; **175**: 299–305.
8. Gras P, Truant S, Boige V, Ladrat L, Rougier P, Pruvot FR, et al. Prolonged complete response after GEMOX chemotherapy in a patient with advanced fibrolamellar hepatocellular carcinoma. *Case Rep Oncol* 2012; **5**: 169–72. doi: 10.1159/000338242
9. Brandt DJ, Johnson CD, Stephens DH, Weiland LH. Imaging of fibrolamellar hepatocellular carcinoma. *AJR Am J Roentgenol* 1988; **151**: 295–9. doi: 10.2214/ajr.151.2.295
10. Friedman AC, Lichtenstein JE, Goodman Z, Fishman EK, Siegelman SS, Dachman AH. Fibrolamellar hepatocellular carcinoma. *Radiology* 1985; **157**: 583–7. doi: 10.1148/radiology.157.3.2997835
11. Ichikawa T, Federle MP, Grazioli L, Madariaga J, Nalesnik M, Marsh W. Fibrolamellar hepatocellular carcinoma: imaging and pathologic findings in 31 recent cases. *Radiology* 1999; **213**: 352–61. doi: 10.1148/radiology.213.2.r99nv31352
12. Ichikawa T, Federle MP, Grazioli L, Marsh W. Fibrolamellar hepatocellular carcinoma: pre- and posttherapy evaluation with CT and MR imaging. *Radiology* 2000; **217**: 145–51. doi: 10.1148/radiology.217.1.r00se46145
13. McLarney JK, Rucker PT, Bender GN, Goodman ZD, Kashitani N, Ros PR. Fibrolamellar carcinoma of the liver: radiologic-pathologic correlation. *Radiographics* 1999; **19**: 453–71. doi: 10.1148/radiographics.19.2.g99mr09453
14. Stevens WR, Johnson CD, Stephens DH, Nagorney DM. Fibrolamellar hepatocellular carcinoma: stage at presentation and results of aggressive surgical management. *AJR Am J Roentgenol* 1995; **164**: 1153–8. doi: 10.2214/ajr.164.5.7717223
15. Powers C, Ros PR, Stoupis C, Johnson WK, Segel KH. Primary liver neoplasms: MR imaging with pathologic correlation.

- Radiographics* 1994; **14**: 459–82. doi: [10.1148/radiographics.14.3.8066263](https://doi.org/10.1148/radiographics.14.3.8066263)
16. Ichiki Y, Sugio K, Baba T, Mizukami M, Oga T, Takenoyama M, et al. Mediastinal metastasis from a fibrolamellar hepatocellular carcinoma: report of a case. *Surg Today* 2010; **40**: 360–4. doi: [10.1007/s00595-009-4035-4](https://doi.org/10.1007/s00595-009-4035-4)
  17. Tsilivlidis B, Huet E, Lubrano J, Lacaze L, Lestrat JP, François A, et al. Late supra-diaphragmatic lymph node recurrence following resection of a fibrolamellar hepatocarcinoma: an unusual case. *Surg Radiol Anat* 2010; **32**: 123–7. doi: [10.1007/s00276-009-0564-1](https://doi.org/10.1007/s00276-009-0564-1)
  18. Uchino K, Tateishi R, Shiina S, Kanda M, Masuzaki R, Kondo Y, et al. Hepatocellular carcinoma with extrahepatic metastasis: clinical features and prognostic factors. *Cancer* 2011; **117**: 4475–83. doi: [10.1002/cncr.25960](https://doi.org/10.1002/cncr.25960)
  19. Corrigan K, Semelka RC. Dynamic contrast-enhanced MR imaging of fibrolamellar hepatocellular carcinoma. *Abdom Imaging* 1995; **20**: 122–5.
  20. Meyers AB, Towbin AJ, Serai S, Geller JI, Podberesky DJ. Characterization of pediatric liver lesions with gadoxetate disodium. *Pediatr Radiol* 2011; **41**: 1183–97. doi: [10.1007/s00247-011-2148-6](https://doi.org/10.1007/s00247-011-2148-6)
  21. Campos JT, Sirlin CB, Choi JY. Focal hepatic lesions in Gd-EOB-DTPA enhanced MRI: the atlas. *Insights Imaging* 2012; **3**: 451–74. doi: [10.1007/s13244-012-0179-7](https://doi.org/10.1007/s13244-012-0179-7)
  22. Winston CB, Schwartz LH, Fong Y, Blumgart LH, Panicek DM. Hepatocellular carcinoma: MR imaging findings in cirrhotic livers and noncirrhotic livers. *Radiology* 1999; **210**: 75–9. doi: [10.1148/radiology.210.1.r99ja1975](https://doi.org/10.1148/radiology.210.1.r99ja1975)
  23. Hui MS, Choi WM, Perng HL, Chen LK, Yang KC, Chen TJ. Fibrolamellar hepatocellular carcinoma—an atypical MR manifestation. *Hepatogastroenterology* 1998; **45**: 514–17.
  24. Blachar A, Federle MP, Ferris JV, Lacomis JM, Waltz JS, Armfield DR, et al. Radiologists' performance in the diagnosis of liver tumors with central scars by using specific CT criteria. *Radiology* 2002; **223**: 532–9. doi: [10.1148/radiol.2232010801](https://doi.org/10.1148/radiol.2232010801)